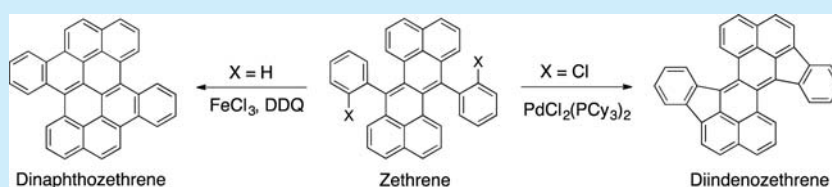


## Dinaphthozethrene and Diindenzethrene: Synthesis, Structural Analysis, and Properties

Ya-Chu Hsieh,<sup>†</sup> Tsun-Cheng Wu,<sup>†</sup> Jen-Yi Li,<sup>†</sup> Yi-Ting Chen,<sup>‡</sup> Ming-Yu Kuo,<sup>\*,§</sup> Pi-Tai Chou,<sup>\*,‡</sup> and Yao-Ting Wu<sup>\*,†</sup><sup>†</sup>Department of Chemistry, National Cheng Kung University, No. 1 Ta-Hsueh Road, 70101 Tainan, Taiwan<sup>‡</sup>Department of Chemistry, National Taiwan University, No. 1, Sec. 4, Roosevelt Road, 10617 Taipei, Taiwan<sup>§</sup>Department of Applied Chemistry, National Chi Nan University, No. 1 University Road, 54561 Puli, Nantou, Taiwan

## S Supporting Information



**ABSTRACT:** Zethrene-based condensed arenes dinaphthozethrene and diindenzethrene were synthesized by oxidative cyclodehydrogenation and palladium-catalyzed cyclization of 7,14-diarylzethrenes, respectively. Their structures were analyzed by X-ray crystallography. The photophysical and electrochemical properties of these compounds were investigated.

Dibenzo[*de,mn*]naphthacene (zethrene) **1** (Figure 1) is an important class of compounds for chemists and material

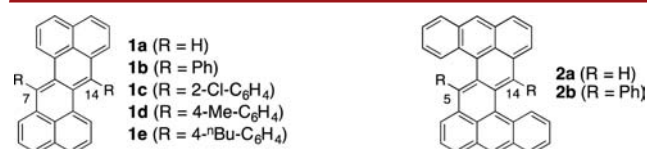
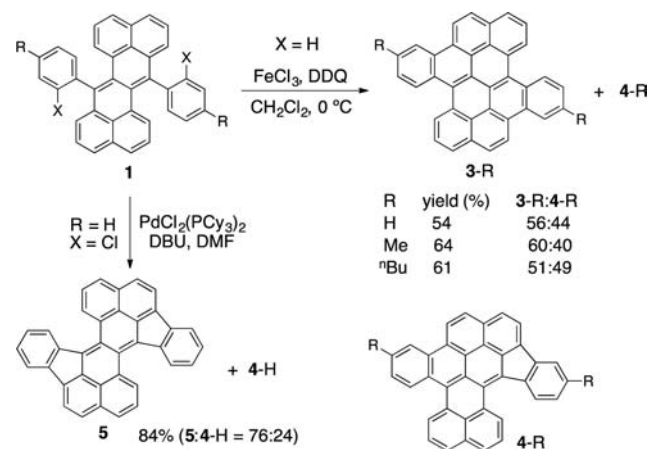


Figure 1. Zethrenes **1** and dibenzozethrenes **2**.

scientists.<sup>1</sup> The central two six-membered rings in **1** cannot account for the aromaticity associated with the Kekulé structure, and their weak aromaticity has been confirmed experimentally.<sup>1e</sup> Experimental investigations have also demonstrated that zethrene and its derivatives have potential applications in electroluminescent devices<sup>1a</sup> and organic transistors.<sup>1c,2</sup> Additionally, a recent study of zethrene **1** and dibenzozethrene **2** revealed that substituents and  $\pi$ -conjugation influence their biradical properties.<sup>3</sup> Unlike closed-shell disubstituted **1b** and **2b**, the parent compounds **1a** and **2a** are singlet open-shell biradicals,<sup>4</sup> and the latter has a much stronger biradical character than the former.<sup>5</sup> In light of this information, the chemistry of zethrene-based condensed arenes dinaphthozethrene and diindenzethrene was explored.

Zethrene-based condensed arenes were prepared from 7,14-diarylzethrenes. Scheme 1 presents the synthetic approaches. Due to the very low aromaticity of the central two six-membered rings in **1**, the central  $\pi$ -bonds can be regarded as a 1,3-butadienyl moiety. Therefore, 7,14-diphenylzethrene **1b** may undergo photochemical cyclization to form dinaphthozethrene **3-H**, in a manner similar to the synthesis of phenanthrene from 1,2-diphenylethene.<sup>6</sup> However, only precipitates, but not **3-H**, were

Scheme 1. Synthesis of Condensed Arenes **3** and **5**

obtained. Presumably, this unsatisfactory result was caused by photo-oxygenation-induced polymerization.<sup>7</sup> Fortunately, the oxidative cyclodehydrogenation of **1b** mediated by iron(III) chloride and DDQ generated a mixture of **3-H** and **4-H**, which could not be separated by simple chromatography or crystallization due to their poor solubility in common organic solvents. Although both products were not fully characterized by NMR spectroscopy, very small amounts of them were separately obtained by using a preparative HPLC, and they were identified as having equal molar masses.<sup>9</sup> The introduction of two additional alkyl side chains sufficiently increased solubility.

Received: March 6, 2016

Published: April 5, 2016

Alkyl-substituted **3** and **4** were separated by crystallization. Compounds **3** are more stable than 7,14-diarylzethrenes. The solutions of **3**-Me and **3**-<sup>n</sup>Bu in CDCl<sub>3</sub> under dark and aerobic conditions did not produce new signals in their <sup>1</sup>H NMR spectra, even after several months.

Palladium-catalyzed intramolecular arylations of 7,14-di(2-chlorophenyl)zethrene (**1c**) formed **5** and 4-H (≈3:1 ratio) with a total yield of 84%. The pure form of the former product was obtained by crystallization from the mixture. Although 4-H cannot be isolated, some signals in the <sup>1</sup>H NMR spectra of **3**-H/4-H and **5**/4-H are identical. Similar to the solution of **3**, the solution of **5** in CDCl<sub>3</sub> was highly stable for at least several months. Notably, **5** is a distinctive fragment of some unusual fullerenes such as C<sub>68</sub>,<sup>10a</sup> C<sub>76</sub>,<sup>10b</sup> and C<sub>78</sub>.<sup>10c</sup>

Single crystals of **3**-Me and **5** suitable for X-ray crystallographic analysis were grown by the diffusion of MeOH into their solutions in benzene and CH<sub>2</sub>Cl<sub>2</sub>, respectively, at room temperature. **3**-<sup>n</sup>Bu has a better solubility than **3**-Me, and its crystals were easier to grow, but its molecules were highly disordered in the solid and unsuitable for X-ray crystallography. Dinaphthozethrene **3**-Me adopts a nonplanar structure with C<sub>2</sub> symmetry, and its degree of twisting, measured as the dihedral angle between the mean square planes of two periphery naphthalene moieties (B/C and B'/C'), was determined as 27.2° (Figure 2).<sup>11</sup> The twisting of the structure is caused by the

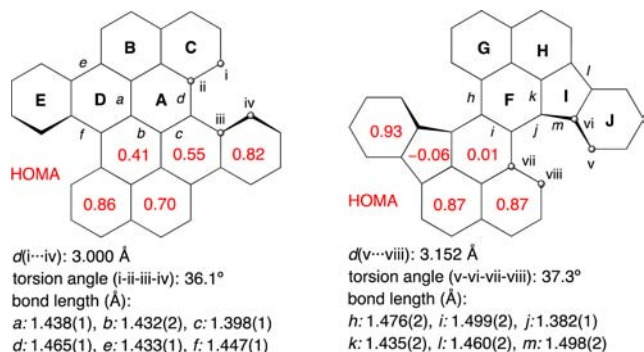


**Figure 2.** Selected structural data and HOMA indices of **3**-Me and **5**. Values were obtained by averaging the symmetry-related data based on X-ray crystallography.

bay region clashes, which are identified by their large torsion angle (36°, determined by i-ii-iii-iv) and the short distance between nonbonded atoms i and iv (3.00 Å), which is even smaller than the sum of the van der Waals radii of two carbon atoms (3.40 Å).<sup>12</sup> The bond distances in zethrene **1a** and its counterpart in **3**-Me differ significantly. The latter has shorter bonds *a* and *b* than the former by approximately 3.5 pm but a longer bond *c* by around 2.0 pm. Bonds *e* (1.43 Å) and *f* (1.45 Å) are shorter than a regular single bond (1.48 Å) that connects two aryl rings.<sup>13</sup> This fact may suggest that ring **D** exhibits some aromaticity and is involved in the  $\pi$ -system of the backbone. Indeed, it and other six-membered rings in **3**-Me have moderate to high aromaticity, based on HOMA (harmonic oscillator model of aromaticity) analyses,<sup>14</sup> from which values of 1 and 0 indicate aromaticity and nonaromaticity, respectively. These geometric findings and results concerning aromaticity demonstrate that the zethrene backbone in **3**-Me is similar to that in the biradical compound **2a**, which has a shortened bond *b* (1.450 Å), an elongated bond *c* (1.367 Å), and some aromaticity in ring **A** (HOMA = 0.28). However, **3** is closed-shell, as confirmed by

theoretical studies<sup>15</sup> and electron spin resonance measurements of **3**-<sup>n</sup>Bu. Line broadening was not observed in the <sup>1</sup>H NMR spectra of **3**-Me and **3**-<sup>n</sup>Bu.

C<sub>2</sub>-symmetric diindenozethrene **5**<sup>16</sup> is twisted with a dihedral angle between the mean square planes of two periphery naphthalene moieties (rings **G/H** and **G'/H'**) of 35.9°. The torsion angle at the fjord region (v-vi-vii-viii) and the distance between nonbonded atoms v and viii were determined to be 37.3° and 3.152 Å, respectively. Notably, the bond *i* [1.499(2) Å] in **5** is much longer than that in **1b** [1.467(4) Å], and a regular single bond connects two alkenyl moieties (1.451 Å).<sup>17</sup> This information demonstrates that the interaction between the two alkenyl moieties (bonds *j*) is negligible. HOMA analysis reveals that ring **F** is nonaromatic, whereas rings **G**, **H**, and **J** have very high aromaticity. Based on the results of these analyses, the zethrene fragment in **5** is more similar to that in **1b** than to that in **1a**. Compound **5** with a closed-shell ground state was theoretically<sup>15</sup> and experimentally verified.

In its solid form, **3**-Me stacks in columns along the *c* axis, but the molecules slip from side to side (Figure 3). The effective  $\pi/\pi$

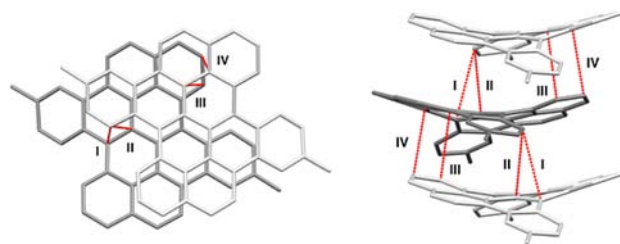


**Figure 3.** Crystal packing in **3**-Me along the *b* axis (left) and the *c* axis (right). Only carbon atoms are shown for clarity. Nonbonded carbon-carbon distances in Å: (I) 3.363, (II) 3.305, (III) 3.306, and (IV) 3.268.

surface overlap is mostly between their dibenzo[*g,p*]chrysene moieties. Within a columnar stack, the distance between any two adjacent molecules is around 3.8 Å, and the shortest carbon-carbon nonbonded distance is 3.268 Å. Molecules of **5** also form columnar stacks along the *c* axis, as presented in Figure 4. Any two adjacent molecules within a column exhibit perfect face-to-face overlap with a distance of 3.924 Å.

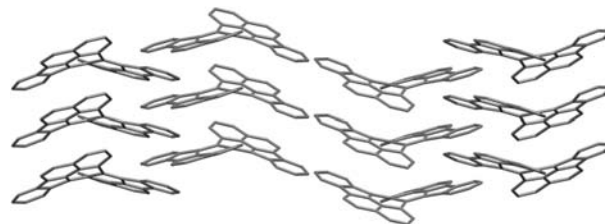


**Figure 4.** Crystal packing in **5** along the *c* axis. Only carbon atoms are shown for clarity.

Electrochemical properties of condensed arenes **3**-<sup>n</sup>Bu and **5** were examined using cyclic voltammetry. The cyclic voltammogram of **3**-<sup>n</sup>Bu includes signals of one irreversible oxidation and one reversible reduction, whereas that of **5** includes three redox waves with one irreversible oxidation and two reversible reduction peaks (Table 1). The irreversibility of an oxidation wave generally reveals the low thermodynamic stability of the cation species. It has to be emphasized that the area ratio of the oxidation wave to the reduction signal of **3**-<sup>n</sup>Bu was determined to be 2.5:1. Therefore, this oxidation wave should be taken

Table 1. Selected Physical Properties of Dinaphthozethrene 3-*n*-Bu and Diindenoazethrene 5<sup>a</sup>

	$\lambda_{\text{abs}}$ (nm)	$\lambda_{\text{em}}$ (nm)	$\tau_f$ (ns)	QY <sup>b</sup>	$E_{1/2}^{\text{ox}}$ (V)	$E_{1/2}^{\text{red}}$ (V)	$E_g^{\text{P}}$ (eV)	$E_g^{\text{E}}$ (eV)	$\sigma_{\text{max}}$ (GM)
1a	543	574	7.18	0.599	0.30	−1.69, −2.06 <sup>c</sup>	2.12	2.00	373 at 530 nm
2a	592	683	3.16	0.051	0.22, 0.55 <sup>c</sup>	−1.58, −1.83 <sup>c</sup>	1.95	1.81	4323 at 530 nm
3- <i>n</i> -Bu	492	506	1.74	0.31	0.16 <sup>c</sup>	−2.00	2.44	2.16	253 at 450 nm
5	625	645	0.75	$3.1 \times 10^{-3}$	0.31 <sup>c</sup>	−1.27, −1.59	1.75	1.58	274 at 590 nm

<sup>a</sup>Electrochemical and photophysical properties of 3-*n*-Bu and 5 were measured in CH<sub>2</sub>Cl<sub>2</sub>.  $\lambda_{\text{abs}}$ : absorption peak wavelength.  $\lambda_{\text{em}}$ : photoluminescence wavelength.  $\tau_f$ : fluorescence lifetime.  $E_{1/2}^{\text{ox}}$  and  $E_{1/2}^{\text{red}}$  are half-wave potentials of the oxidative and reductive waves measured in CH<sub>2</sub>Cl<sub>2</sub>, respectively, with a scan rate of 50 mV/s and potentials vs Fc/Fc<sup>+</sup> couple.  $E_g^{\text{P}}$  is the optical energy gap derived from the lowest energy absorption onset in the absorption spectrum.  $E_g^{\text{E}}$ : electrochemical HOMO–LUMO gap.  $\sigma_{\text{max}}$ : maximum TPA cross section. Physical properties of 1a and 2a were taken from ref 4. <sup>b</sup>QY: fluorescence quantum yield (reference for 3-*n*-Bu: rhodamine 6G in methanol,  $\lambda_{\text{ex}}$  = 450 nm; reference for 5: LDS821 in chloroform,  $\lambda_{\text{ex}}$  = 550 nm). <sup>c</sup>For an irreversible wave, the potential was determined by its onset value.

account for a nearly single two-electron transfer. The first reduction potential of 5 (−1.27 V vs Fc/Fc<sup>+</sup>) is much lower than those of 3-*n*-Bu (−2.00 V), 1a (−1.69 V), and 2a (−1.58 V), indicating that 5 has a low LUMO energy level, which is mainly responsible for its having the smallest electrochemical HOMO–LUMO gap ( $E_g^{\text{E}}$  = 1.58 eV).<sup>18</sup> Additionally, the energy gaps ( $E_g^{\text{E}}$ ) of C<sub>76</sub> (1.64 eV), C<sub>78</sub> (1.72 and 1.47 eV), and their distinctive fragment 5 are comparable, and they are much smaller than those of C<sub>60</sub> (2.32 eV) and C<sub>70</sub> (2.22 eV).<sup>19</sup>

Photophysical properties of 3-*n*-Bu and 5 in CH<sub>2</sub>Cl<sub>2</sub> (10  $\mu$ M) at room temperature were studied (Table 1 and Supporting Information). These compounds are orange and blue, respectively. The longest wavelength absorption of 3-*n*-Bu ( $\epsilon$  =  $2.94 \times 10^4$  M<sup>−1</sup> cm<sup>−1</sup>) was observed as a relatively sharp band centered at 492 nm, whereas 5 ( $\epsilon$  =  $3.99 \times 10^3$  M<sup>−1</sup> cm<sup>−1</sup>) exhibited a weak and a broad transition from 430 to 710 nm centered at 625 nm. The absorption and emission bands of 5 are red-shifted from those of 3-*n*-Bu by approximately 140 nm. Both the absorption and emission bands of 3-*n*-Bu are blue-shifted from those of the fragment 1a as the standard, whereas those of 5 were shifted bathochromically. Consequently, their optical HOMO–LUMO gaps ( $E_g^{\text{P}}$ ) follow the order 3-*n*-Bu > 1a > 5. Notably, 5, cyclopenta[*hi*]aceanthrylene 6,<sup>20,21</sup> and dicyclopenta[*de,mn*]-naphthacene 7<sup>21</sup> (Figure 5) have similar physical properties, including two reversible reduction potentials, a low electrochemical band gap, and an extremely low fluorescence quantum yield.

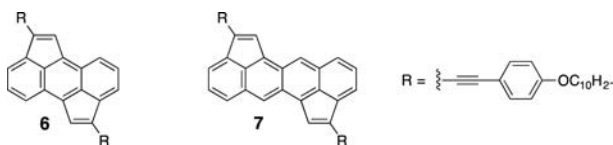


Figure 5. Cyclopenta[*hi*]aceanthrylene 6, and dicyclopenta[*de,mn*]-naphthacene 7.

The nonlinear optical properties of 3-*n*-Bu and 5 were measured using a method based on two-photon-induced fluorescence with excitation wavelengths of 900–1420 nm, in which measurements were not perturbed by one-photon absorption. The TPA cross sections ( $\sigma_{\text{max}}$ ) of 3-*n*-Bu and 5 are smaller than those of 1a and 2a (Table 1).

Interestingly, 3-*n*-Bu and 5 have 36  $\pi$ -electrons, but their electrochemical and photophysical properties differ remarkably. To gain insight into the origin of these differences, their structures and frontier molecular orbital profiles were calculated at the B3LYP/6-31G\*\* level using Gaussian 09.<sup>22</sup> The optimized geometries for the compounds are highly consistent with the structures obtained by X-ray crystallography (see Supporting

Information). Figure 6 demonstrates that two *n*-butyl groups of 3-*n*-Bu have no effect on either the HOMO or the LUMO.

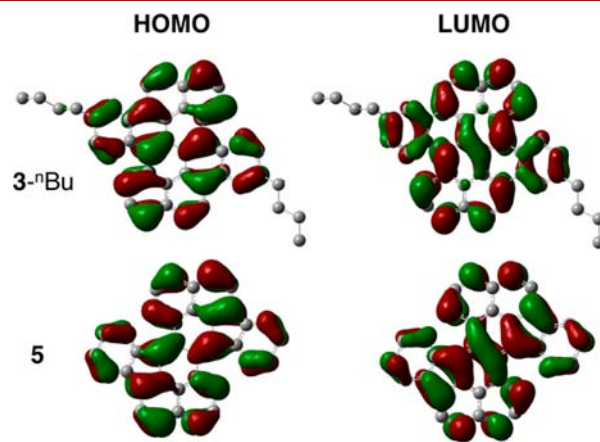


Figure 6. HOMOs and LUMOs of 3-*n*-Bu and 5 calculated at the B3LYP/6-31G\*\* level.

Although the extent of efficient  $\pi$ -conjugations of 3-*n*-Bu and 5 cannot be easily distinguished using the molecular orbital profiles, the computational outcomes based on TDDFT at the B3LYP/6-31G\*\* level agree with the tendency of the experimental results obtained herein. The longest absorption bands,  $\lambda_{\text{abs}}$ , attributable to HOMO–LUMO transitions ( $S_0 \rightarrow S_1$  bands) of 3-*n*-Bu and 5 were determined to be 500 and 650 nm, respectively (see Supporting Information). The extremely low fluorescence of 5 should not be caused by the symmetry-forbidden HOMO-to-LUMO transition<sup>23</sup> because its values of the measured absorption coefficient and the calculated oscillator strength ( $f$  = 0.34) cannot be ignored.

In conclusion, simple synthetic methods for preparing highly stable dinaphthozethrene and diindenoazethrene from 7,14-diarylethrenes have been developed. Although both compounds have 36  $\pi$ -electrons, their different geometries strongly influence their aromaticity and physical properties. Due to its low HOMO–LUMO energy gap and perfect molecular aggregation, 5 has potential applications as organic field-effect transistors and/or fullerene-like electron acceptors in solar cells. These applications are currently being examined.

## ■ ASSOCIATED CONTENT

### Supporting Information

The Supporting Information is available free of charge on the ACS Publications website at DOI: 10.1021/acs.orglett.6b00637.



Complete ref 22, experimental procedures, characterization data, and computational studies (PDF)  
X-ray crystallographic data for 3-Me (CIF)  
X-ray crystallographic data for 5 (CIF)

## AUTHOR INFORMATION

### Corresponding Authors

\*E-mail: mykuo@ncnu.edu.tw.

\*E-mail: chop@ntu.edu.tw.

\*E-mail: ytwuchem@mail.ncku.edu.tw.

### Notes

The authors declare no competing financial interest.

## ACKNOWLEDGMENTS

This work was supported by the Ministry of Science and Technology of Taiwan. We thank Prof. Sue-Lein Wang and Ms. Pei-Lin Chen (National Tsing Hua University, Taiwan) for the X-ray structure analyses.

## REFERENCES

- (1) (a) Sun, Z.; Wu, J. *J. Org. Chem.* **2013**, *78*, 9032. (b) Hibi, D.; Kitabayashi, K.; Shimizu, A.; Umeda, R.; Tobe, Y. *Org. Biomol. Chem.* **2013**, *11*, 8256. (c) Shan, L.; Liang, Z.; Xu, X.; Tang, Q.; Miao, Q. *Chem. Sci.* **2013**, *4*, 3294. (d) Sun, Z.; Huang, K.-W.; Wu, J. *Org. Lett.* **2010**, *12*, 4690. (e) Wu, T.-C.; Chen, C.-H.; Hibi, D.; Shimizu, A.; Tobe, Y.; Wu, Y.-T. *Angew. Chem., Int. Ed.* **2010**, *49*, 7059. (f) Umeda, R.; Hibi, D.; Miki, K.; Tobe, Y. *Org. Lett.* **2009**, *11*, 4104. (g) Umeda, R.; Hibi, D.; Miki, K.; Tobe, Y. *Pure Appl. Chem.* **2010**, *82*, 871.
- (2) Theoretical studies indicate that the HOMO–LUMO energy gap of the parent zethrene is almost identical to that of pentacene. See: Ruiz-Morales, Y. *J. Phys. Chem. A* **2002**, *106*, 11283.
- (3) For recent reviews on biradicals, see: (a) Abe, M. *Chem. Rev.* **2013**, *113*, 7011. (b) Morita, Y.; Nishida, S. In *Stable Radicals*; Hicks, R. G., Ed.; Wiley: Chichester, 2010; p 81. (c) Sun, Z.; Zeng, Z.; Wu, J. *Acc. Chem. Res.* **2014**, *47*, 2582. (d) Kubo, T. *Chem. Lett.* **2015**, *44*, 111. (e) Kubo, T. *Chem. Rec.* **2015**, *15*, 218. (f) Zeng, Z.; Shi, X.; Chi, C.; López Navarrete, J. T.; Casado, J.; Wu, J. *Chem. Soc. Rev.* **2015**, *44*, 6578. (g) Miyoshi, H.; Nobusue, S.; Shimizu, A.; Tobe, Y. *Chem. Soc. Rev.* **2015**, *44*, 6560.
- (4) Hsieh, Y.-C.; Fang, H.-Y.; Chen, Y.-T.; Yang, R.; Yang, C.-I.; Chou, P.-T.; Kuo, M.-Y.; Wu, Y.-T. *Angew. Chem., Int. Ed.* **2015**, *54*, 3069.
- (5) For details of other  $\pi$ -extended zethrene derivatives such as heptazethrenes, octazethrenes, and dibenzoheptazethrenes, see: (a) Sun, Z.; Huang, K.-W.; Wu, J. *J. Am. Chem. Soc.* **2011**, *133*, 11896. (b) Li, Y.; Heng, W.-K.; Lee, B. S.; Aratani, N.; Zafra, J. L.; Bao, N.; Lee, R.; Sung, Y. M.; Sun, Z.; Huang, K.-W.; Webster, R. D.; Navarrete, J. T. L.; Kim, D.; Osuka, A.; Casado, J.; Ding, J.; Wu, J. *J. Am. Chem. Soc.* **2012**, *134*, 14913. (c) Sun, Z.; Lee, S.; Park, K. H.; Zhu, X.; Zhang, W.; Zheng, B.; Hu, P.; Zeng, Z.; Das, S.; Li, Y.; Chi, C.; Li, R.-W.; Huang, K.-W.; Ding, J.; Kim, D.; Wu, J. *J. Am. Chem. Soc.* **2013**, *135*, 18229. (d) Hu, P.; Lee, S.; Herng, T. S.; Aratani, N.; Gonçalves, T. P.; Qi, Q.; Shi, X.; Yamada, H.; Huang, K.-W.; Ding, J.; Kim, D.; Wu, J. *J. Am. Chem. Soc.* **2016**, *138*, 1065.
- (6) (a) Mattay, J.; Griesbeck, A. *Photochemical Key Steps in Organic Synthesis*; Wiley-VCH: Weinheim, 1994. (b) Mallory, F. B.; Mallory, C. W. *Organic Reactions* **1984**, *30*, 1.
- (7) For the photo-oxygenation of zethrene, see: Clar, E. *Chem. Ber.* **1955**, *88*, 1520.
- (8) The original Rathore's condition ( $\text{CF}_3\text{CO}_2\text{H}$  and DDQ) did not give a satisfactory result: Zhai, L.; Shukla, R.; Rathore, R. *Org. Lett.* **2009**, *11*, 3474.
- (9) Under similar conditions, a fluorene derivative can be generated from diarylmethane by ring closure of the central five-membered ring. For details, see ref 8.
- (10) (a) Zólyomi, V.; Peterlik, H.; Bernardi, J.; Bokor, M.; László, I.; Koltai, J.; Kurti, J.; Knapfer, M.; Kuzmany, H.; Pichler, T.; Simon, F. *J. Phys. Chem. C* **2014**, *118*, 30260. (b) Ioffe, I. N.; Goryunkov, A. A.; Tamm, N. B.; Sidorov, L. N.; Kemnitz, E.; Troyanov, S. I. *Angew. Chem., Int. Ed.* **2009**, *48*, 5904. (c) Kemnitz, E.; Troyanov, S. I. *Mendeleev Commun.* **2010**, *20*, 74.
- (11) With respect to the relative conformations of the two bay regions, this compound should have two conformers,  $\text{C}_2$ -3 and  $\text{C}_7$ -3. Theoretical studies at the B3LYP/6-31G\*\* level indicated that  $\text{C}_2$ -3-H is more stable than  $\text{C}_7$ -3-H by 3.5 kcal/mol. The barrier to the interconversion between two conformers was determined to be 11.0 kcal/mol (see Supporting Information).
- (12) Pauling, L. *The Nature of the Chemical Bond*, 3rd ed.; Cornell University Press: Ithaca, NY, 1960.
- (13) (a) Dewar, M. J. S.; Schmeising, H. N. *Tetrahedron* **1959**, *5*, 166. The single bond in perylene was determined to be 1.474 Å. For details, see: (b) Ranganathan, A.; Kulkarni, G. U. *Proc. - Indian Acad. Sci., Chem. Sci.* **2003**, *115*, 637.
- (14) (a) Kruszewski, J.; Krygowski, T. M. *Tetrahedron Lett.* **1972**, *13*, 3839. For a review on HOMA, see: (b) Krygowski, T. M.; Cyrański, M. *K. Chem. Rev.* **2001**, *101*, 1385.
- (15) The biradical character indices ( $y_0$ ) of  $\text{C}_2$ -3-"Bu,  $\text{C}_7$ -3-"Bu,  $\text{C}_2$ -5, and  $\text{C}_7$ -5 were examined using the spin-projected unrestricted Hartree–Fock method. The first three have a closed-shell ground state, whereas  $\text{C}_7$ -5 is a singlet biradical molecule with an index value of 0.38.
- (16) According to theoretical studies at the B3LYP/6-31G\*\* level,  $\text{C}_2$ -5 is 7.4 kcal/mol more stable than  $\text{C}_7$ -5. The barrier to the interconversion is 11.6 kcal/mol (see Supporting Information).
- (17) The crystal structure of *trans,trans*-1,3,5,7-octatetraene indicates that the carbon–carbon bond lengths starting from the chain end are 1.336, 1.451, 1.327, and 1.451 Å. See: Baughman, R. H.; Kohler, B. E.; Levy, I. J.; Spangler, C. *Synth. Met.* **1985**, *11*, 37.
- (18) One reviewer suggested that the low LUMO energy level of 5 is most likely caused by it having a vinylogous biindenylidene subunit. For details, see: (a) Brunetti, F. G.; Gong, X.; Tong, M.; Heeger, A. J.; Wudl, F. *Angew. Chem., Int. Ed.* **2010**, *49*, 532. (b) Iyoda, M.; Otani, H.; Oda, M. *Angew. Chem., Int. Ed. Engl.* **1988**, *27*, 1080.
- (19) Yang, Y.; Arias, F.; Echegoyen, L.; Chibante, L. P. F.; Flanagan, S.; Robertson, A.; Wilson, L. J. *J. Am. Chem. Soc.* **1995**, *117*, 7801.
- (20) Dang, H.; Levitus, M.; Garcia-Garibay, M. A. *J. Am. Chem. Soc.* **2002**, *124*, 136.
- (21) Wood, J. D.; Jellison, J. L.; Finke, A. D.; Wang, L.; Plunkett, K. N. *J. Am. Chem. Soc.* **2012**, *134*, 15783.
- (22) Frisch, M. J.; et al. *Gaussian 09*, revision A.1; Gaussian, Inc.: Wallingford, CT, 2009.
- (23) The extremely low fluorescence of some arenes with 4n  $\pi$ -electrons is caused by the symmetry-forbidden HOMO-to-LUMO transition. For selected examples, see: (a) Blood, C. T.; Linstea, R. P. *J. Chem. Soc.* **1952**, 2263. (b) Kawase, T.; Konishi, A.; Hirao, Y.; Matsumoto, K.; Kurata, H.; Kubo, T. *Chem. - Eur. J.* **2009**, *15*, 2653. (c) Wu, T.-C.; Tai, C.-C.; Tiao, H.-C.; Chang, Y.-T.; Liu, C.-C.; Li, C.-H.; Huang, C.-H.; Kuo, M.-Y.; Wu, Y.-T. *Chem. - Eur. J.* **2011**, *17*, 7220.